ISSN 2706-655X Vol.6, Issue 4: 127-132, DOI: 10.25236/IJFET.2024.060420

Structural Parameter Optimization Study of Online Pipeline Flame Arresters

Hui Liu, Chuanhong Wang, Ming Li, Lixin Zhou, Jinghong Dai, Yongliang Zeng, Ying Li

PetroChina Southwest Oil & Gas Field Company Chongqing Gas Mine, Chongqing, 400120, China

Abstract: *In gas transmission stations, conventionally designed pipeline flame arresters are prone to clogging, affecting the normal venting of natural gas. Therefore, it is necessary to optimize the parameters of flame arresters. Modeling and analysis of online pipeline flame arresters were conducted using Ansys Workbench software. The results indicate that the quenching distance of the flame increases linearly with the increase in the aperture ratio; the explosion pressure and flame speed at the front of the arrester generally decrease as the aperture ratio increases; the explosion pressure at the front of the arrester increases with the thickness of the flame arresting core, while the flame speed decreases with the increase in the thickness of the flame arresting unit. Thus, the optimal aperture ratio for online pipeline flame arresters is determined to be 0.4, with a thickness of 120mm.*

Keywords: *Flame arrester; Numerical simulation; Parameter optimization*

1. Introduction

A pipeline flame arrester is a safety device used to prevent the propagation of flames. It consists of a solid material (flame arresting element) that allows gas to pass through and has many fine channels or gaps. The gaps or channels of the flame arresting element are required to be as small as possible. When the flame enters the arrester, it is divided into many small flame streams by the flame arresting element. Due to heat transfer (gas cooling) and wall effects, the flame streams are quenched.[1]

In practical operations, conventionally designed flame arresters are prone to clogging, affecting the normal venting of natural gas at production sites. To address the clogging issue, it is necessary to optimize the structural parameters of the arrester to avoid equipment defects and reduce clogging failures.

Currently, extensive research and practical applications on the quenching theory have been carried out by scholars domestically and internationally. These studies not only provide theoretical support for the design of flame arresters but also lay a solid foundation for this research.

2. Characteristics of Online Pipeline Flame Arresters

The models and specifications of flame arresters installed on different vent pipelines vary, but the basic requirement is that the effective flow area of the flame arrester must be greater than or equal to the flow area of the vent pipeline. The following calculation is based on a flame arrester for a Dn80 vent pipeline, as shown in Figure 1. The flame arrester has a thickness of 130mm, with 18 openings, and a small hole radius of 9mm.[2]

Figure 1: Structural Diagram of Online Flame Arrester

ISSN 2706-655X Vol.6, Issue 4: 127-132, DOI: 10.25236/IJFET.2024.060420

3. Optimization Analysis Method for Online Flame Arrester

Based on Ansys Workbench software, a simulation calculation model of the online flame arrester was established according to Figure 1. Before constructing the simulation calculation model of the online flame arrester, a series of reasonable assumptions were made to ensure the accuracy and computational efficiency of the model.

First, the effect of radiative heat transfer was neglected because the working environment of the online flame arrester is typically not a high-temperature radiation environment, making this assumption reasonable. Secondly, to simplify the calculation process, the influence of body forces was ignored, which helps to reduce the computational load while maintaining accuracy. Furthermore, the Soret effect and Dufour effect were not considered, meaning that viscous dissipation effects were assumed to be zero. This is an important assumption as it greatly simplifies the mathematical model, making the computational process more efficient. Lastly, it was assumed that the combustion process involves only a single-step reaction, based on the working principle and practical application scenarios of the online flame arrester.[3]

During the model construction, a series of governing equations were involved. These equations are crucial for describing the physical processes within the online flame arrester, including the mass conservation equation, momentum conservation equation, and energy conservation equation. The mass conservation equation describes the mass distribution and flow conditions within the online flame arrester, the momentum conservation equation describes the motion state of the fluid within the arrester, and the energy conservation equation reflects the temperature field changes inside the arrester.

3.1 Mass Conservation Equation

The mathematical expression of the mass conservation equation is shown in Equation (1).

$$\frac{\partial}{\partial t}\int\int\int_{V}\rho dxdydz+\int\int_{A}\rho v\cdot ndA=0 \tag{1}$$

In the equation, VVV represents the control volume and AAA represents the control surface.

Its differential form of the equation is shown in Equation (2).

$$\frac{\partial\rho}{\partial t}+u\frac{\partial(\rho u)}{\partial x}+v\frac{\partial(\rho v)}{\partial y}+w\frac{\partial(\rho w)}{\partial z}=0 \tag{2}$$

In the equation, u, v, and w represent the velocity components in the x-axis, y-axis, and z-axis directions, respectively.

3.2 Momentum Conservation Equation

For compressible viscous fluids, the momentum conservation equation is shown in Equation (3).

$$\frac{\partial}{\partial t}\left(\rho\vec{v}\right)+\nabla\cdot\left(\rho\vec{v}\vec{v}\right)=-\nabla P+\nabla\cdot\left(\vec{\tau}\right) \tag{3}$$

In the equation, ρ represents the gas density, and τ represents the stress tensor.

3.3 Energy Conservation Equation

The energy conservation equation is shown in Equation (4).

$$\frac{\partial(\rho T)}{\partial t}+\frac{\partial}{\partial x_i}(\rho u_i T)=\frac{\partial}{\partial x_i}\left(\frac{\lambda}{C_p}\frac{\partial T}{\partial x_i}\right)+\frac{1}{C_p}\frac{\partial P}{\partial t}+\frac{h_c}{C_p}R_{燃,A} \tag{4}$$

In the equation, h_c represents the heat of combustion.

ISSN 2706-655X Vol.6, Issue 4: 127-132, DOI: 10.25236/IJFET.2024.060420

Simultaneously, choosing an appropriate model is crucial for in-depth research on the numerical simulation of the combustion process. In this study, the standard k-ε model was used to describe turbulent motion, the species transport model was used to track the concentration changes of chemical species, and the EBU-Arrhenius combustion model was used to characterize the variation of turbulent combustion rates during the combustion process[5-6]. The selection of these three models aims to comprehensively and accurately simulate the physical and chemical phenomena during combustion.

During the solving process, the PISO algorithm from the pressure-velocity coupling algorithms was chosen, with a time step of 10−510^{-5}10−5 seconds[7]. For the initial conditions, it was assumed that there was a burnt region near the closed end of the circular pipe, with its temperature set to 2267K, while the unburnt region's temperature was set to 300K. This setup is based on the actual combustion process, where the high-temperature state of the burnt region triggers the combustion reaction, and the low-temperature state of the unburnt region provides the necessary reactants and energy for combustion.[4]

4. Analysis of Calculation Results

4.1 Analysis of Deflagration Flame Quenching Process

When the flame disperses into the various microporous channels of the flame arresting unit, it rapidly loses heat due to the strong surface effects of the channels, ultimately leading to a temperature drop and extinguishment. Generally, the flame extinguishes when the temperature drops to 1700K. Therefore, for the methane-air mixture, this study uses the 1700K isotherm as the position of the flame front and maps the distribution of the flame front position over time, as shown in Figure 2. At around t=140t = 140t=140 ms, the propagation distance reaches its maximum. Afterward, the flame propagation distance remains almost unchanged, indicating that the flame propagation has been interrupted and the flame has been quenched. The quenching distance is defined as the maximum distance that the flame can propagate within the flame arresting unit.

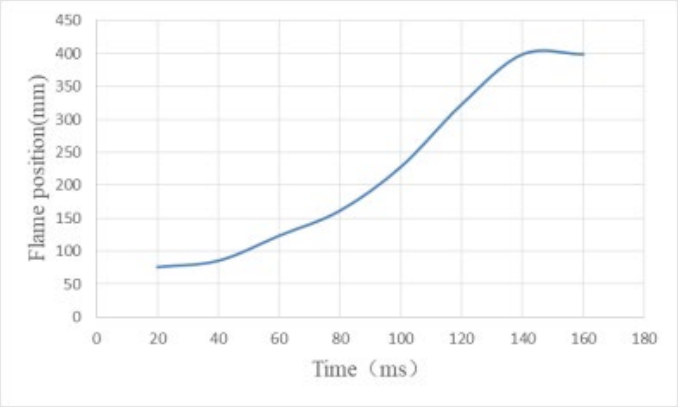

Figure 2: Curve of Flame Position Variation Over Time

4.2 Influence of Aperture Ratio on Flame Quenching Distance

In this study, the venting channels of the flame arresting element are composed of 18 symmetrical cylinders. To determine the effect of venting hole diameter on flame arresting performance and to enhance the adaptability of the research results, the parameter aperture ratio (γ) is introduced to evaluate the impact of venting hole diameter on flame arresting performance.

$$\gamma=\frac{d}{D} \tag{5}$$

In the equation, d represents the diameter of the venting hole, and D represents the inner diameter of the pipeline.

For methane gas at stoichiometric concentration, there is a specific relationship between the quenching distance of the flame within the flame arrester and the aperture ratio. Experimental results show that the quenching distance tends to be linearly distributed, which means that as the aperture ratio decreases, the flame propagation distance within the flame arrester is more significantly restricted. To

ISSN 2706-655X Vol.6, Issue 4: 127-132, DOI: 10.25236/IJFET.2024.060420

describe this relationship more accurately, a linear model was used to process the data, as shown in Equation (6). This model serves as the basis for the quantitative analysis of flame arrester performance.

Additionally, the research results indicate that reducing the aperture ratio can effectively quench methane flames within the flame arrester. This finding is of significant importance for optimizing the design of flame arresters. By reducing the aperture ratio, the efficiency of flame quenching within the arrester can be increased, thereby enhancing its performance in preventing flame propagation.

$$L = 29.273\gamma + 3.33 \tag{6}$$

In the equation, L represents the flame quenching distance, and γ represents the aperture ratio.

4.3 Influence of Aperture Ratio on Front-End Explosion Pressure and Flame Arresting Speed

In this section of the simulation study, the gas propagation process within the pipeline flame arrester system was analyzed, with a focus on the variations in front-end explosion pressure and flame arresting speed. These analyses are crucial for understanding the working principles and performance evaluation of flame arresters.

First, the flame arresting speed within the pipeline flame arrester with different aperture ratios was analyzed. The results show that the flame arresting speed tends to follow an exponential distribution. This finding suggests that the flame arresting speed is not only influenced by the aperture ratio but also potentially related to the interaction mechanisms between the flame and the flame arresting elements. As the aperture ratio increases, the flame propagation speed within the flame arrester gradually decreases, reflecting the regulatory effect of the aperture ratio on flame arresting performance.

Secondly, the explosion pressure at the front end of the flame arrester was thoroughly studied. The results indicate that the explosion pressure generally decreases with the increase in aperture ratio, showing a linear relationship. This finding provides a basis for quantitatively assessing the impact of aperture ratio on flame arrester performance.

Based on the above analyses, the following conclusions can be drawn: within the pipeline flame arrester system, both the explosion pressure and flame arresting speed are influenced by the aperture ratio. As the aperture ratio increases, the explosion pressure decreases, and the flame arresting speed reduces. These relationships can be described by linear and exponential functions, as shown in Equations (7) and (8).

The relationship between explosion pressure and aperture ratio is as follows:

$$P = -0.8745\gamma + 0.502 \tag{7}$$

In the equation, P represents the explosion pressure, and γ represents the aperture ratio.

The relationship between flame arresting speed and aperture ratio is as follows:

$$V = -36.16\exp\left(4\gamma^2\right) + 127.4 \tag{8}$$

In the equation, V represents the flame arresting speed, and γ represents the aperture ratio.

4.4 Influence of Flame Arresting Core Thickness on Front-End Explosion Pressure and Flame Arresting Speed

In the numerical calculations, the pipeline parameters and aperture ratio values were kept consistent, while the thickness of the flame arresting core was varied from 60mm to 200mm. Through this series of simulation calculations, the results indicate that the explosion pressure increases with the thickness of the flame arresting core, showing a linear relationship (as shown in Equation (9)). This means that increasing the thickness of the flame arresting core can enhance the flame arrester's ability to withstand explosion pressure.

Secondly, the flame arresting speed decreases as the thickness of the flame arresting core increases, exhibiting a quadratic relationship (as shown in Equation (10)). This finding suggests that while increasing the thickness of the flame arresting core can improve the flame arrester's resistance to explosion pressure, it also reduces the flame arresting speed. Therefore, in the design of flame arresters, it is necessary to balance and trade off between these two factors.

ISSN 2706-655X Vol.6, Issue 4: 127-132, DOI: 10.25236/IJFET.2024.060420

From the above analysis, it can be seen that the performance of the flame arrester is closely related to the thickness of the flame arresting core. By adjusting the thickness of the flame arresting core, the explosion resistance capability and flame arresting speed of the flame arrester can be effectively regulated. This provides useful reference and guidance for the design optimization and practical application of flame arresters.

The relationship between explosion pressure and flame arresting core thickness is as follows:

$$P = 0.0006l + 0.0797 \tag{9}$$

In the equation, P represents the explosion pressure, and l represents the flame arresting core thickness.

The relationship between flame arresting speed and flame arresting core thickness is as follows:

$$V = 62.72 - 0.196l + 4.12\times10^{-4}l^2 \tag{10}$$

In the equation, VVV represents the flame arresting speed, and l represents the flame arresting core thickness.

By studying the quenching laws within the pipeline flame arrester system, it was found that the flame quenching distance increases linearly with the increase in aperture ratio. The explosion pressure and flame arresting speed at the front end of the flame arrester generally decrease as the aperture ratio increases. Additionally, the explosion pressure at the front end of the flame arrester increases with the increase in flame arresting core thickness, while the flame arresting speed decreases as the thickness increases.

Although increasing the flame arresting core thickness and decreasing the aperture ratio can more effectively quench the flame, the pressure drop at both ends of the flame arrester also increases accordingly. An efficient flame arrester should not only have good flame arresting performance but also minimize the resistance to fluid flow. Therefore, considering all factors, the optimal aperture ratio is determined to be 0.4, with a thickness of 120mm.

5. Conclusion

The flame quenching distance increases linearly with the increase in aperture ratio. This finding indicates that the aperture ratio is a key factor influencing the flame quenching distance. Therefore, it is necessary to reasonably control the aperture ratio in the design of flame arresters to achieve effective flame quenching.

The explosion pressure at the front end of the flame arrester decreases with the increase in aperture ratio and increases with the increase in flame arresting core thickness. This finding reveals the impact of aperture ratio and flame arresting core thickness on the flame arrester's ability to withstand explosion pressure. By adjusting these parameters, the performance of the flame arrester can be optimized to improve its resistance to explosion pressure.

The flame arresting speed generally decreases with the increase in aperture ratio and decreases with the increase in flame arresting core thickness. This indicates that the design of flame arresters needs to comprehensively consider the effects of aperture ratio and flame arresting core thickness on flame arresting speed to achieve fast and effective flame arresting.

The optimal aperture ratio for the online pipeline flame arrester is determined to be 0.4, with a thickness of 120mm. This parameter combination ensures that the flame arrester can withstand explosion pressure while achieving fast and effective flame arresting within the pipeline.

References

[1] Peng F, Liu H, Cai W. Combustion diagnostics of metal particles: a review [J]. Measurement Science and Technology, 2023, 34(4): 042002.
[2] Zheng Jinlei. Research on the flame-retardant performance testing and characteristics of pipeline flame arresters [D]. Jiangsu: China University of Mining and Technology, 2022.
[3] Liu Xi, Liu Shijie. Design of gas transmission pipelines and venting systems in natural gas stations [J]. Shanghai Gas, 2021, (06): 12-14+26.
[4] Hu Chunming. Study on the propagation and quenching of methane/air premixed flame in a flat slit

ISSN 2706-655X Vol.6, Issue 4: 127-132, DOI: 10.25236/IJFET.2024.060420

[J]. Liaoning Chemical Industry, 2008, (06): 375-377+419.
[5] Jiang Deming. Combustion and emission of internal combustion engines[M]. Xi'an: Xi'an Jiaotong University, 2002.
[6] Zhou Kaiyuan, Li Zongfen, Zhou Zijin. Experimental study on the quenching effect of corrugated plate flame arresters on deflagration flames [J]. Journal of the University of Science and Technology of China, 1997(04): 77-82.
[7] Wen Xiaoping, Yu Minggao, Xie Maozhao, et al. Dynamic propagation and quenching characteristics of gas deflagration flames in narrow slits [J]. Journal of China Coal Society, 2013, 38(S2): 383-387.